



LETTER • OPEN ACCESS

Projected evolution of droughts and human exposure in the contiguous United States under SSP5-8.5: a regional downscaling perspective

To cite this article: Leyuan Zhang et al 2025 Environ. Res. Lett. 20 094021

View the article online for updates and enhancements.

You may also like

- <u>Drought variability in the eastern Australia</u> and New Zealand summer drought atlas (ANZDA, CE 1500–2012) modulated by the Interdecadal Pacific Oscillation Jonathan G Palmer, Edward R Cook, Chris S M Turney et al.
- Comment on 'Drought variability in the eastern Australia and New Zealand summer drought atlas (ANZDA, CE 1500–2012) modulated by the Interdecadal Pacific Oscillation' Tessa R Vance, Jason L Roberts, Chris T Plummer et al.
- The feasibility of reconstructing hydroclimate over West Africa using treering chronologies in the Mediterranean region

Boniface O Fosu, Edward R Cook, Michela Biasutti et al.



ENVIRONMENTAL RESEARCH

LETTERS



OPEN ACCESS

RECEIVED

2 December 2024

REVISED

21 July 2025

ACCEPTED FOR PUBLICATION 28 July 2025

PUBLISHED

5 August 2025

Original content from this work may be used under the terms of the Creative Commons Attribution 4.0 licence.

Any further distribution of this work must maintain attribution to the author(s) and the title of the work, journal citation and DOI.



LETTER

Projected evolution of droughts and human exposure in the contiguous United States under SSP5-8.5: a regional downscaling perspective

Leyuan Zhang¹, Hannah J Rubin¹, Rong-You Chien¹, Joshua S Fu^{1,2,*}, Deeksha Rastogi², Shih-Chieh Kao³, and Moetasim Ashfaq²

- Department of Civil and Environmental Engineering, University of Tennessee, Knoxville, TN 37996, United States of America
- ² Computational Sciences and Engineering Division, Oak Ridge National Laboratory, Oak Ridge, TN 37831, United States of America
- ³ Environmental Sciences Division, Oak Ridge National Laboratory, Oak Ridge, TN 37831, United States of America
- * Author to whom any correspondence should be addressed.

E-mail: jsfu@utk.edu

Keywords: climate change, drought, CMIP6, regional downscaling, soil moisture deficits, population exposure Supplementary material for this article is available online

Abstract

The increasingly unpredictable and extreme weather patterns under a warming climate underscore the urgency of accurate regional assessments of future drought risk. This study evaluates the projected drought evolution in the contiguous United States under the high-emission shared socioeconomic pathway 5-8.5 climate scenario for the coming decades. Using a multi-model ensemble of six Coupled Model Intercomparison Project Phase 6 global climate models combined with dynamical downscaling techniques, we analyzed near-term (2020-2039) and mid-term (2040–2059) drought patterns using the self-calibrating palmer drought severity index (ScPDSI), the standardized precipitation index (SPI-12), and the Standardized Precipitation-Evapotranspiration Index (SPEI-12). Results reveal a widespread increase in abnormally dry (D0) and moderate drought (D1) conditions, particularly in urban areas, while severe (D2), extreme (D3), and exceptional (D4) droughts are expected to become less common in many regions. Meanwhile, persistent and intensifying droughts are projected in the western and southwestern U.S., driven by long-term soil moisture deficits. The ScPDSI projects that 1.1 million urban residents will be affected by D0 conditions in 2050, while SPI-12 suggests a decrease in the total affected populations after 2040. ScPDSI indicates prolonged droughts in the West, and SPI-12 captures transient variability. Although the total drought-exposed population is expected to decrease, urban areas will continue to bear a greater burden, particularly for mild droughts (D0, D1). These findings highlight a shift toward more frequent mild droughts, fewer severe droughts, and persistent drying in the Southwest, emphasizing the need for region-specific adaptation strategies.

1. Introduction

Drought is one of the most persistent and disruptive climate hazards across the contiguous United States (CONUSs), with far-reaching consequences for water availability, agriculture, public health, and economic stability (Heim 2002, Leeper *et al* 2022, Sugg *et al* 2020, Zhang *et al* 2020). Recent events—such as the 2000, 2002, 2006, and 2011–2013 droughts—have

become more intense and spatially variable (Rippey 2015), heightening risks of wildfires, crop losses, water shortages, and health impacts concerns (Covich *et al* 2009, Chang *et al* 2016, Littell *et al* 2016, Chiang *et al* 2018, Falloon *et al* 2018). Drought-related disasters have caused more than \$31 billion in damages in the U.S. between 1980 and 2023 (Smith 2020), underscoring the need of improving drought prediction and management.

Drought indices offer quantitative tools for characterizing different aspects of drought, including precipitation deficits, evapotranspiration, and soil moisture (Mishra and Singh 2010). The standardized precipitation index (SPI-12) over a 12 month scale (SPI-12) remains a widely used indicator of long-term meteorological drought, due to its simplicity and comparability across regions (McKee et al 1993, Hu et al 2015). It is independent of the magnitude of mean precipitation, which makes it comparable across different climate zones and time scales (Agnew 2000, Li et al 2020). However, SPI-12 does not account for temperature-driven water loss, limiting its effectiveness in warming regions (Hoffmann et al 2020). The Standardized Precipitation Evapotranspiration Index (SPEI-12) addresses this by incorporating potential evapotranspiration (PET), offering a more climatesensitive measure of drought (Vicente-Serrano et al 2010). However, its sensitivity depends on how PET is calculated. While the Thornthwaite method is commonly used, it often overestimates drought severity in warmer conditions due to its reliance on temperature alone (Hayes et al 2012, Beguería et al 2014). In contrast, the Penman–Monteith method accounting for solar radiation, humidity, and wind speed—offers a more physically grounded alternative (Zhao et al 2023).

In addition to precipitation and temperature, soil moisture dynamics are critical for assessing drought severity. The self-calibrating palmer drought severity index (ScPDSI) accounts for soil moisture balance and local water-holding capacity, making it suitable for hydrological and agricultural drought assessments (Palmer 1965, Dai and Zhao 2017, Zhong et al 2019). While SPI and SPEI are more sensitive to shortterm variability, ScPDSI offers insight into long-term drought persistence (Karl 1983). Soil moisture-based indices have been shown to more effectively capture hydrological and agricultural drought risk than those based on precipitation alone (Vicente-Serrano et al 2011, Wang et al 2017a). The U.S. Drought Monitor (USDM) also combines SPI, PDSI, and other metrics to support drought classification and decisionmaking (Svoboda et al 2002).

While historical precipitation and temperature trends are well documented for most of the U.S. (McEnery et al 2005), future drought projections require high-resolution climate models that capture fine-scale atmospheric and land–surface interactions. The Coupled Model Intercomparison Project Phase 6 (CMIP6) global climate model (GCM) outputs provide standardized future projections, incorporating shared socioeconomic pathways (SSPs) with representative concentration pathways to assess climate impacts under different radiative forcing levels (Eyring et al 2016, O'Neill et al 2016). The SSP5-8.5 scenario is widely applied to explore the upper-bound

climate impacts. However, the coarse resolution (~110 km) and inherent biases of GCM outputs limit their applicability for regional analyses (Hao et al 2018b, Mülmenstädt and Wilcox 2021). Also, high-resolution climate projections are essential for regional drought assessments, especially in topographically complex areas such as the western U.S. (Ashfaq et al 2016). To address this, downscaling techniques are employed to improve resolution (Raju and Kumar 2020, Qiu et al 2022). Statistical downscaling is efficient but depends on empirical relationships that may break down in future climates. In contrast, dynamical downscaling explicitly resolves regional climate processes, such as orographic precipitation and land-atmosphere interactions (Coppola et al 2021, Rastogi et al 2022). In this study, the regional climate model version 4 (RegCM4) is used to refine CMIP6 projections to 4 km resolution, coupled with bias correction using daymet V4 to improve precipitation and temperature accuracy.

This study provides a comprehensive assessment of projected drought trends across CONUS by integrating three key drought indices (SPI-12, SPEI-12, and ScPDSI) to capture precipitation-driven, temperature-driven, and soil moisture-based drought dynamics. By incorporating high-resolution dynamical downscaling with bias correction, we improve the spatial resolution and reliability of future drought projections. Our regional climate-zone-based analysis and multi-model ensemble approach allows for a detailed evaluation of local drought variations. Additionally, by assessing the future drought exposure of urban and rural populations, we also evaluate population exposure to drought, underscoring regional disparities in risk and informing adaptation strategies.

2. Methods and data

2.1. Drought indices and classification

To evaluate the projected drought conditions, we apply three established drought indices: SPI-12, SPEI-12, and ScPDSI. SPI-12, based solely on precipitation, is commonly used for meteorological drought analysis, while SPEI-12 extends this approach by incorporating PET to account for temperature-driven drought stress. Both indices are computed at a 12 month scale to effectively capture prolonged precipitation deficits that influence agricultural production, groundwater recharge, and reservoir storage. This time scale offers a balance between shorter-term variability (e.g. SPI-3, which primarily detects meteorological droughts) and longer-term trends (e.g. SPI-24, which may over-smooth interannual fluctuations), align with widely used methodologies in drought research and ensures comparability with previous studies (Heim 2002, Vicente-Serrano et al 2010,

Table 1. Drought classification for SPI, SPEI, and ScPDSI. (*Adapted from USDM and NOAA).

Label	Category	SPI/SPEI (USDM)	ScPDSI (NOAA)
W4	Exceptional wet	2.0 or greater	5.0 or greater
W3	Extreme wet	1.6–2	4.0-5.0
W2	Severe wet	1.3-1.6	3.0-4.0
W1	Moderate wet	0.8-1.3	2.0-3.0
W0	Abnormally wet	0.5-0.8	1.0-2.0
N	Near normal	-0.5 - 0.5	-1.0 - 1.0
D0	Abnormally drought	-0.8 to -0.5	-2.0 to -1.0
D1	Moderate drought	-1.3 to -0.8	-3.0 to -2.0
D2	Severe drought	-1.6 to -1.3	-4.0 to -3.0
D3	Extreme drought	-2.0 to -1.6	-5.0 to -4.0
D4	Exceptional drought	-2.0 or less	-5.0 or less

Wang et al 2017b). ScPDSI, which incorporates soil moisture balance, is suited to assessing long-term hydrological and agricultural drought. All indices are standardized against the 1980–2019 baseline to ensure consistency in drought characterization and allow consistent comparisons between historical and future conditions. Formulations and methodological details are provided in supplementary text S1 and equations S1–S4. Drought classification follows the USDM and NOAA thresholds (Svoboda et al 2002), with categories D0–D4 representing increasing severity levels (table 1). ScPDSI is used in spatial analyses given its sensitivity to long-term soil moisture anomalies, while SPI-12 and SPEI-12 offer insight into short-term precipitation and temperature effects.

2.2. Dynamical downscaling and bias correction

To improve spatial resolution, we apply dynamical downscaling through RegCM4, which refines coarse CMIP6 GCM outputs (~110 km) to a high-resolution 4 km grid (Rastogi et al 2022). This technique captures fine-scale atmospheric processes—such as orographic precipitation and land-atmosphere interactions-that are often misrepresented in raw GCMs (Giorgi 2019, Coppola et al 2021). In contrast, statistical downscaling relies on empirical relationships between large-scale climate variables and local observations, which may become less reliable under future climate conditions. Also, dynamical downscaling is particularly valuable in topographically complex regions such as the western U.S. (Ashfaq et al 2016). To correct systematic GCM biases, we use quantile mapping with daymet V4—a 1 km gridded observational dataset (Thornton et al 2022). This procedure improves the representation of extremes in semi-arid and mountainous regions and ensures consistency with historical climate conditions (Rastogi et al 2022). The combination of dynamical downscaling and bias correction enhances the accuracy of drought indices, particularly for indices that incorporate temperature-driven evapotranspiration, such as SPEI and ScPDSI. PET was estimated using the VIC model and the Penman–Monteith method (Zhao *et al* 2023). Methodological details, including PET estimation, model selection, and downscaling evaluation, are provided in supplementary texts S1–S3 and table S1. The dataset spans a historical baseline (1980–2019), near-term (2020–2039), and mid-term (2040–2059) period to align with IPCC-relevant climate planning horizons and facilitates comparisons across studies (Rastogi *et al* 2022). And the data are aggregated by the National Centers of Environmental Information (NCEI) climate regions (figure S1) to support regional trend analysis.

2.3. Population exposure analysis

To evaluate the potential population exposure to drought, we used the Global 1 km downscaled population base year and projection grids dataset (SSPs, Revision 01), which provides urban, rural, and total population projections from 2000 to 2100 in 10 year intervals (Jones and O'Neill 2016, Jones et al 2020). Urban and rural classifications follow the Global Human Settlement Layer and census-based definitions, while rural areas include all non-urban grid cells. This enables alignment between demographic patterns and drought severity projections. While this study focuses on SSP5-8.5 to assess the upper bound of future drought severity, future work could examine alternative warming thresholds (e.g. 1.5 °C, 2 °C) to capture broader uncertainties. Population grids were resampled to match the 4 km resolution of the drought indices. This integration of climate and demographic data allows for a spatially explicit assessment of population vulnerability across CONUS. A detailed description of the methods used for regional aggregation and population exposure analysis is available in supplementary text S4.

3. Results

To assess regional drought characteristics, we analyzed SPI-12, SPEI-12, and ScPDSI across the CONUS from 1980 to 2059 (figure 1). SPI-12 indicates a prolonged dry period between 1980 and the early 2000s,

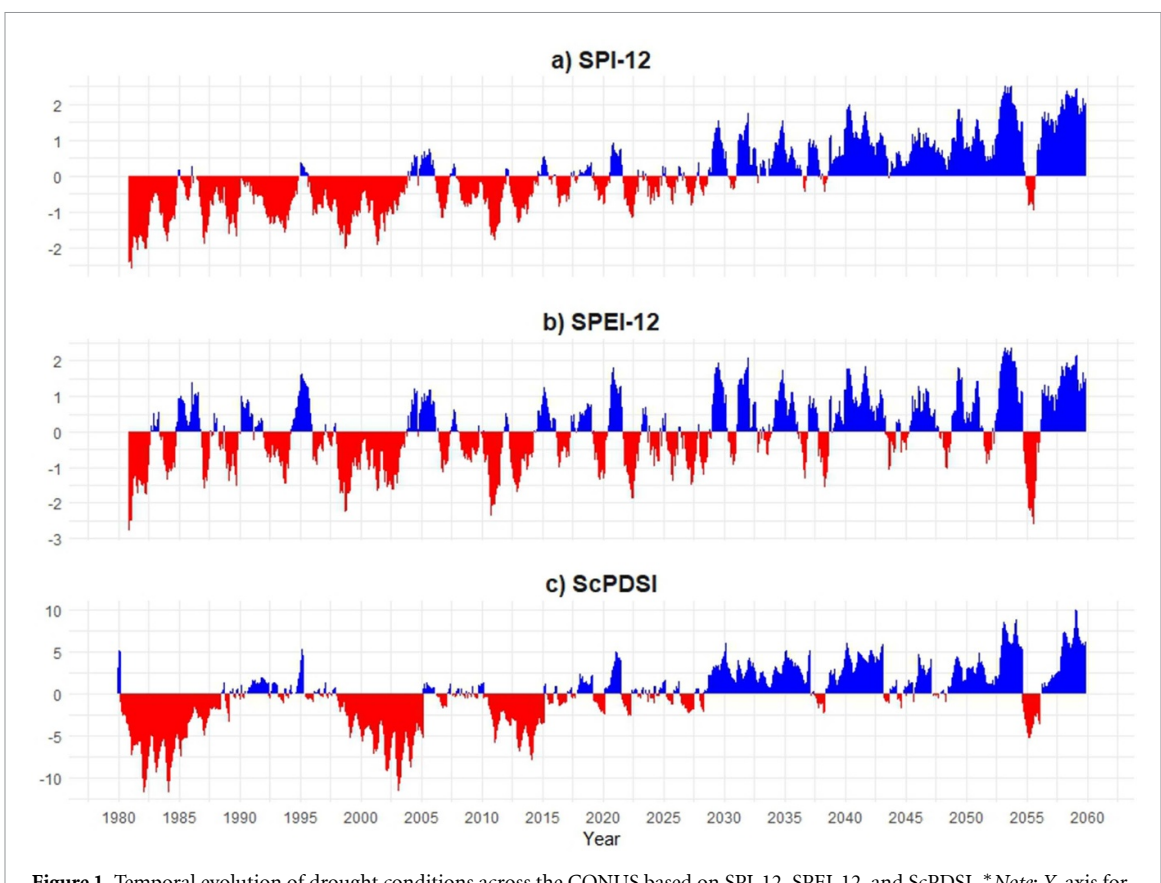


Figure 1. Temporal evolution of drought conditions across the CONUS based on SPI-12, SPEI-12, and ScPDSI. **Note: Y*-axis for ScPDSI differs due to its unique index scale.

with frequent drops below -1, reflecting persistent precipitation deficits. In contrast, SPEI-12 captures shorter drought episodes, as increased evapotranspiration offsets some precipitation deficits. ScPDSI drops below -5 during major droughts in the late 1990s and early 2000s, indicating deep and prolonged soil moisture depletion. Between 2020 and 2059, the indices reveal greater interannual variability, with differing directional trends. SPI-12 indicates a trend toward wetter conditions after 2040, marked by more frequent positive anomalies. While SPEI-12 continues to exhibit strong variability, with droughts intensifying during warmer years due to increased evapotranspiration. ScPDSI shows that the gradual soil moisture recovery in parts of the region reaches values above +5 in some cases after 2030. The contrasting behavior of the indices underscores their complementary strengths in capturing precipitation, temperature, and soil moisture dynamics.

Dynamical downscaling enhances the utility of GCM outputs by incorporating localized atmospheric processes and land–surface interactions, thereby improving the resolution and realism of regional hydroclimate projections. This approach is particularly valuable for assessing drought risk, which is influenced by complex interactions between precipitation, temperature, and soil moisture. To capture

these diverse dimensions, figure 2 illustrates projected regional shifts in drought frequency across the CONUSs for the near-term (2020–2039) and midterm (2040–2059), relative to the historical baseline (1980–2019), based on SPI-12, SPEI-12, and ScPDSI.

The three drought indices show regionally divergent yet complementary patterns across the CONUSs, reflecting their sensitivities to precipitation variability, temperature-driven evaporative demand, and cumulative soil moisture deficits, respectively. To facilitate regional comparisons, we average the combined D1 and D2 proportions across each time period. In the Southwest, including California, Nevada, Arizona, and New Mexico, SPI-12 shows a decline of 5.70 percentage points in D1–D2 drought prevalence from the historical to near-term period and a further 7.40 points decline in the mid-term, indicating a reduction in short-term precipitation deficits. ScPDSI, by contrast, projects increase of 15.45 and 12.10 points across the same two periods, suggesting intensifying long-term drying. SPEI-12 results fall between these two, with respective increases of 1.35 and 2.40 points, likely due to enhanced evaporative demand under rising temperatures despite stable precipitation patterns. In the Northeast, both SPI-12 and SPEI-12 project substantial drought relief, with SPI-12 showing reductions of

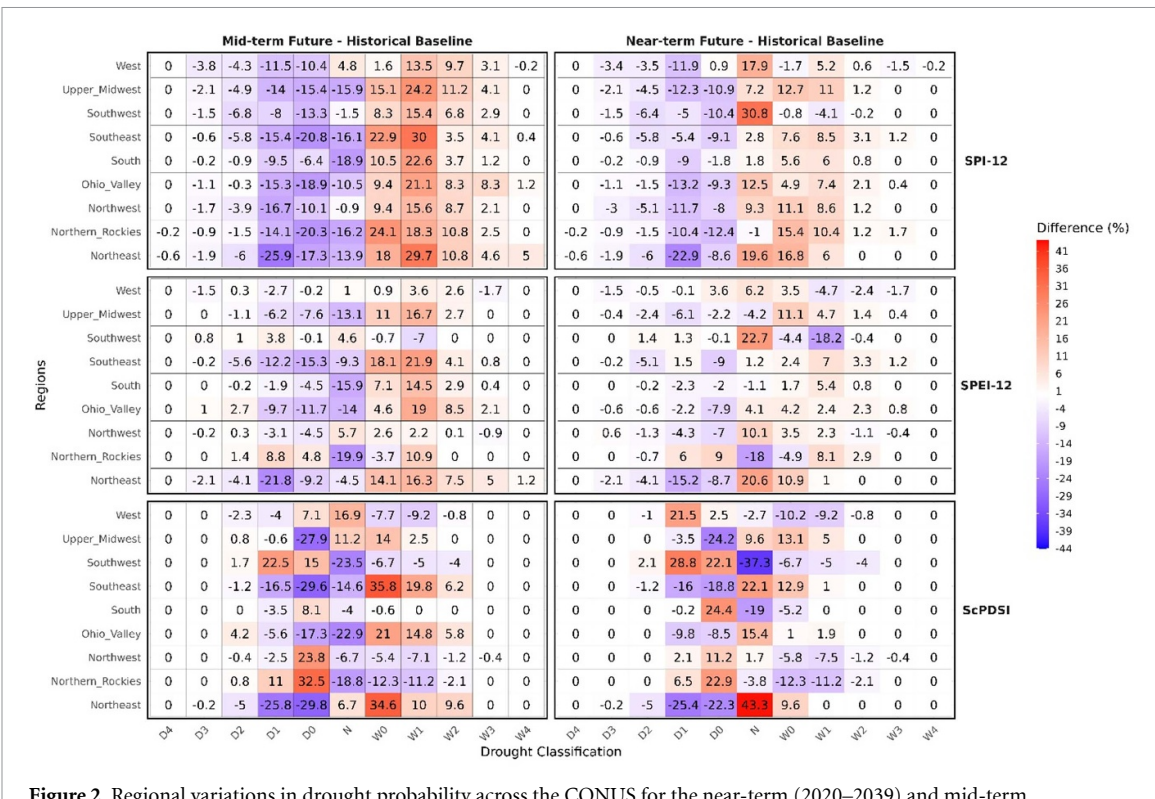


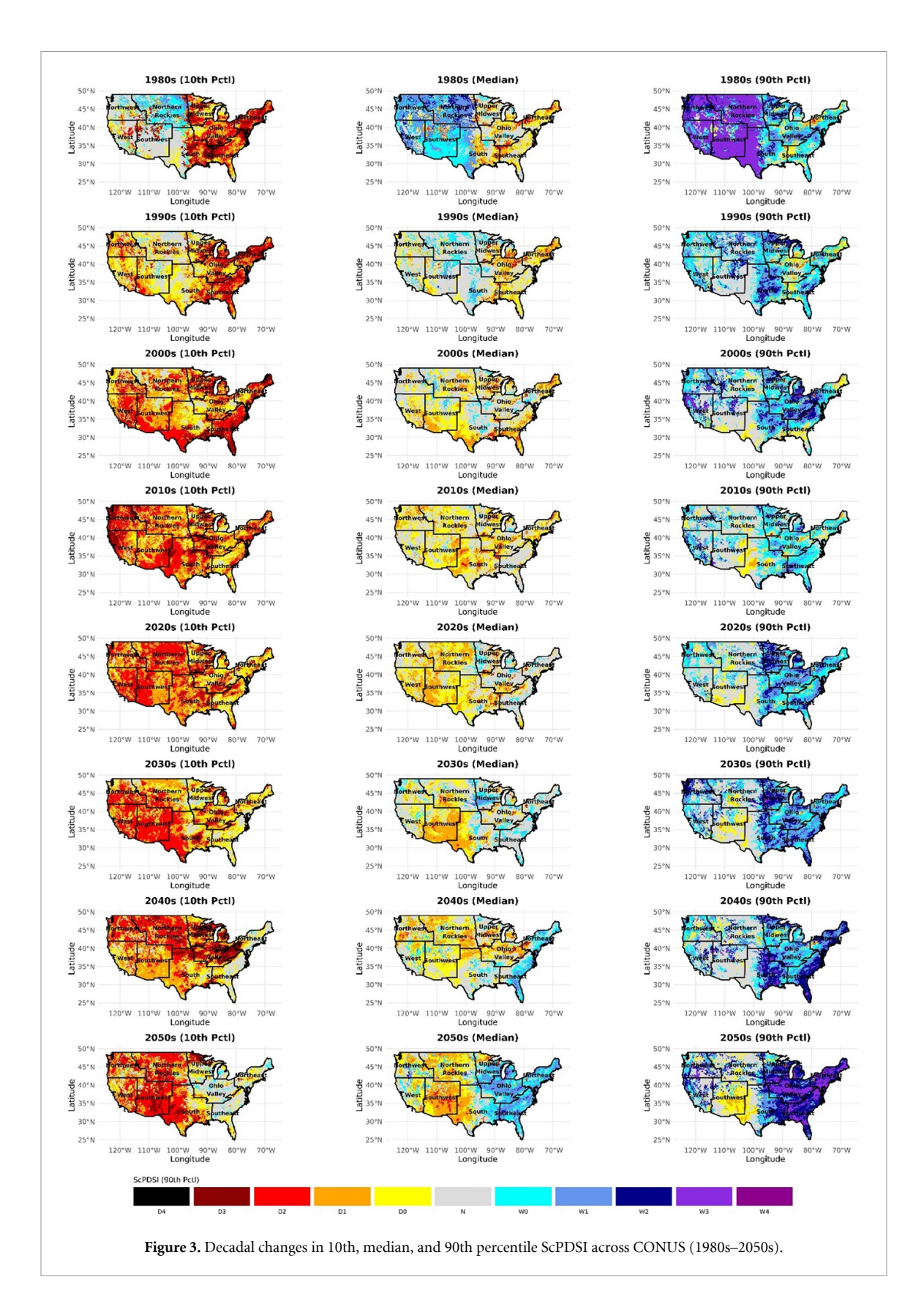
Figure 2. Regional variations in drought probability across the CONUS for the near-term (2020–2039) and mid-term (2040–2059) relative to the historical baseline (1980–2019).

14.45 and 15.95 points, and SPEI-12 showing declines of 9.65 and 12.95 points across the two future periods. Meanwhile, ScPDSI indicates relatively stable long-term moisture conditions, with an increase in near-normal conditions and a decline in both dry and wet extremes. In the Northern Rockies, SPI-12 projects moderate declines of 5.95 and 7.80 points, while SPEI-12 shows increases of 2.65 and 5.10 points, and ScPDSI indicates 5.40 points increase in combined D1 and D2 frequencies by the mid-term. In Ohio Valley, SPI-12 suggests decreases of 7.35 and 7.80 points, SPEI-12 shows smaller reductions of 1.40 and 3.50 points, and ScPDSI indicates a shift from a 9.80-point reduction in D1 in the near-term to a 4.17-point increase in D2 in the mid-term, reflecting a transition toward long-term drying. Overall, SPI-12 frequently indicates decreasing drought severity due to its reliance on precipitation inputs alone, while ScPDSI captures persistent soil moisture deficits that develop over time. SPEI-12 reflects the compounding effects of both temperature and precipitation, often yielding intermediate outcomes. These divergent projections reinforce the value of using multiple indices to provide a more complete understanding of future drought risk across different regions and timescales.

Figure 3 shows a divergent regional trend in climate trends across CONUS from the 1980s–2050s, with increasing drought in the West and increasing wetter conditions in the East. The 10th percentile

ScPDSI maps, which capture extreme dry conditions, indicate that drought was historically confined to the Southwest and Southern Great Plains in the 1980s but has gradually expanded. By the 2000s, severe drought (D3–D4) was widespread across the Southwest, Great Plains, and parts of the Midwest, with California, Nevada, Arizona, and New Mexico showing persistent drying trends. From the 2020s to the 2050s, this pattern intensifies, locking the Southwest and Great Plains into prolonged drought cycles and increasing risks to agriculture, water resources, and wildfires. In contrast, the Northeast and Great Lakes remain relatively resilient, while the Southeast shows emerging drought risks, particularly in Texas, Alabama, Georgia, and Florida.

The median ScPDSI maps, which reflect typical moisture conditions for each decade, show a continued shift toward drier baseline conditions in the West and Great Plains. In these areas, average conditions increasingly fall within the range of moderate to severe drought (D1–D2), indicating that dry conditions previously seen as extreme are becoming the new normal (figure 3). However, the Northeast and Great Lakes show a gradual shift in the opposite direction, with baseline conditions becoming wetter by the mid-century. The Southeast and Midwest show greater variability, with alternating dry and wet periods, making long-term projections more uncertain. Meanwhile, the 90th percentile



ScPDSI maps, which represent extreme wet periods, indicate that the Northeast, Great Lakes, and Ohio Valley are experiencing a sharp increase in extreme wet events (W3–W4), with intense precipitation and flood risks becoming more pronounced from the 2020s onward. The Southeast, particularly along the

Gulf Coast, also sees an increase in extreme wet conditions, likely associated with intensifying tropical storms and hurricanes. In contrast, the Southwest and Great Plains experience a notable decrease in extreme wet periods, reinforcing concerns that these regions are not only drying out but also losing their

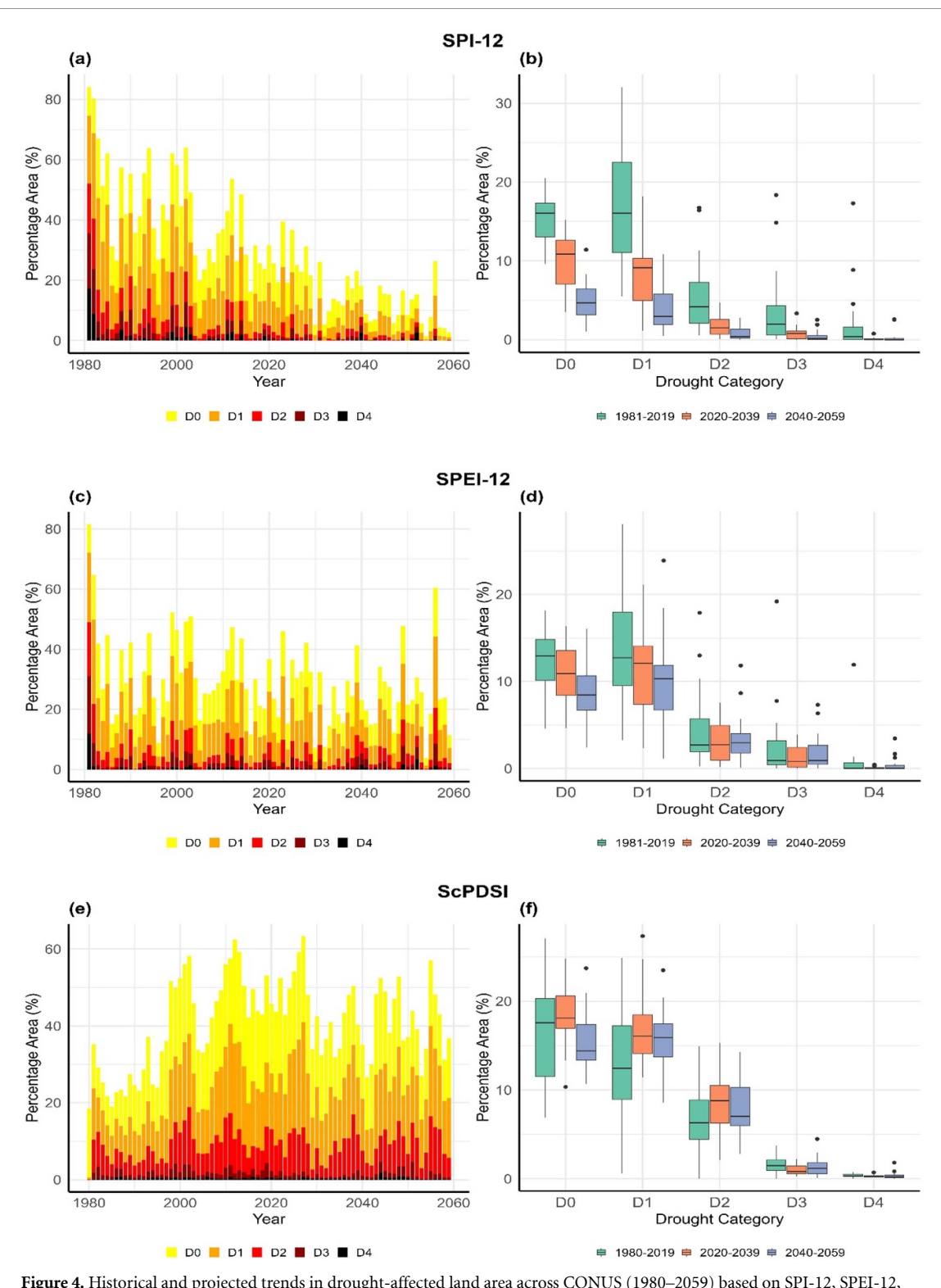


Figure 4. Historical and projected trends in drought-affected land area across CONUS (1980–2059) based on SPI-12, SPEI-12, and ScPDSI. (*Box plots show the median, interquartile range (25th–75th percentiles), whiskers (5th-95th percentiles), and outliers as individual points.).

ability to recover from drought through periodic wet periods.

Figure 4 presents historical and projected changes in the percentage of CONUS affected by different drought categories (D0–D4) from 1980 to 2059, based on SPI-12, SPEI-12, and ScPDSI indices. These visualizations reveal the influence of precipitation

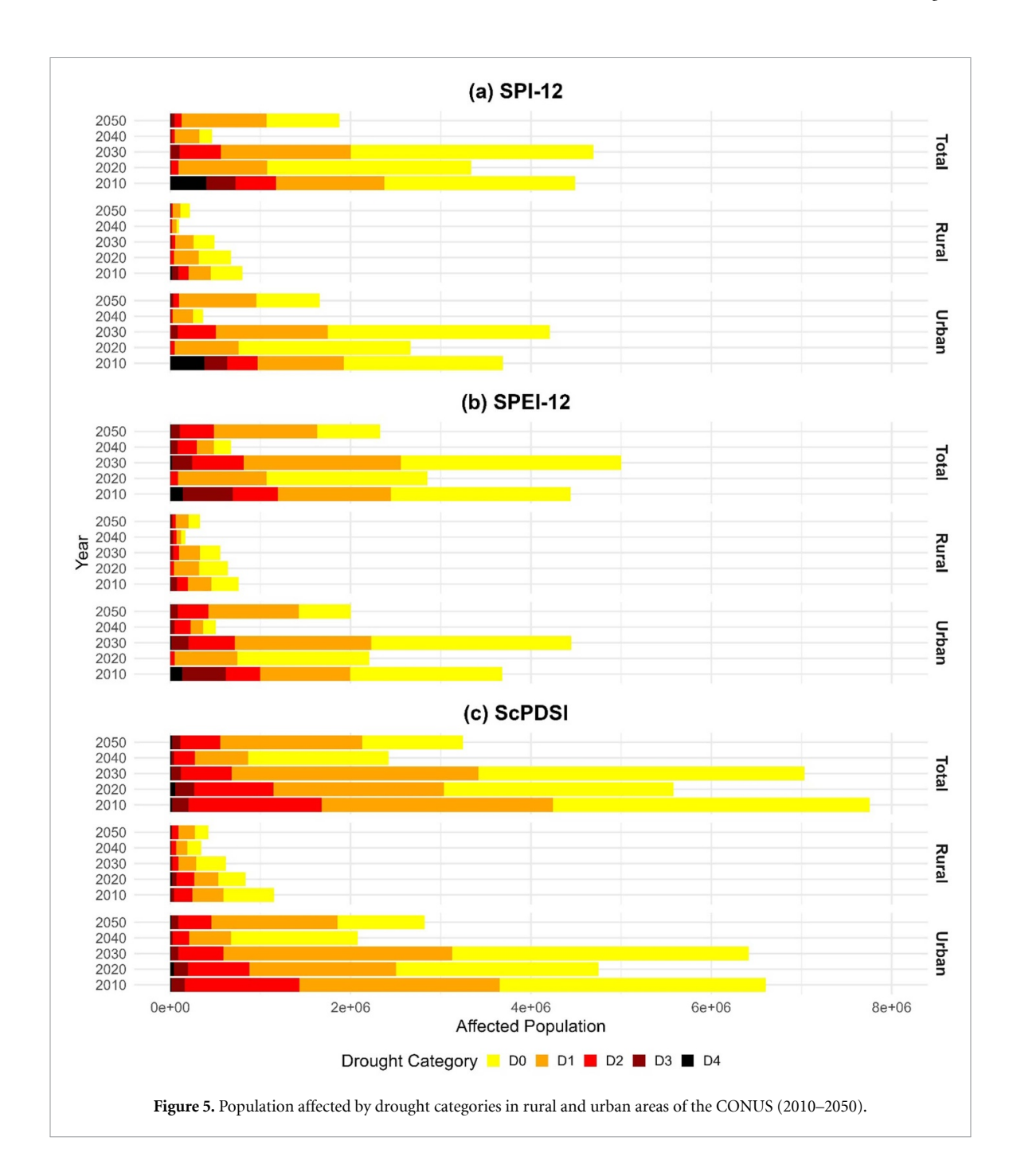
variability, temperature-driven evapotranspiration, and long-term soil moisture trends on future drought conditions under the SSP5-8.5 scenario. The stacked bar plots (figures 4(a), (c) and (e)) show clear temporal trends in drought-affected land area. In SPI-12 (figure 4(a)), the coverage of D1 and D2 decreases from the 1980s onward, with peaks aligning with

major droughts in the late 1980s, early 2000s, and mid-2010s. D3 and D4 remain limited in extent and are not projected to expand significantly, while D0 remains stable, reflecting ongoing short-term precipitation fluctuations. Conversely, SPEI-12 accounts for temperature-driven drying, shows greater year-toyear variability in D1 and D2, indicating that increasing evapotranspiration will intensify drought severity even in years without significant precipitation deficits (figure 4(c)). The area affected by D3 and D4 remains low but sporadic, with peaks indicating years of widespread drying due to extreme heat. ScPDSI presents a different trend, with D0 and D1 coverage increasing significantly after 2020, while D2-D4 remaining relatively stable (figure 4(e)). This indicates a shift towards prolonged dry conditions affecting large portions of the CONUS, rather than episodic severe drought events.

The box plots further explain the statistical distributions across three time periods: 1981-2019 (historical baseline), 2020–2039 (near-term future), and 2040-2059 (mid-term future). For SPI-12, the median D1 and D2 areas decrease in future periods with a reduced interquartile range (IQR), indicating a more consistent decrease in moderate drought coverage (figure 4(b)). However, the whiskers (5th-95th percentiles) and outliers indicate that extreme drought years with widespread impacts remain possible despite the overall downward trend. D3 and D4 continue to affect only a small percentage of the land area, reinforcing that SPI-12-based projections do not suggest an expansion of the most severe drought categories. In contrast, SPEI-12 shows stable median D1 and D2 coverage but with a wider IQR, indicating increased variability in future projections (figure 4(d)). The presence of more outliers in the D2-D4 categories suggests that while overall drought coverage may not increase significantly, extreme heat-driven drying events will lead to years of widespread severe drought. Unlike SPI-12, SPEI-12 shows that moderate to severe droughts may not decrease but will fluctuate more intensely from year to year. ScPDSI projects a clear increase in the median percentage of land affected by D0 and D1 in both future periods, accompanied by a larger IQR (figure 4(f)). This indicates that more of the CONUS will experience persistent abnormally dry or moderate drought conditions. The area affected by D2 remains relatively stable in terms of median values across the three time periods. However, some individual years—particularly around 2030 and 2050 show markedly higher D2 coverage than most historical years (figure 4(e)), consistent with increased interannual variability. These are captured as outliers in the box plot (figure 4(f)) and reflect episodic but widespread severe drought events. It is important to note that these plots represent the spatial extent of drought in a given year, and do not reflect the frequency of drought occurrence at any specific location over time. These projections are consistent with long-term soil moisture deficits expected under a warming climate, where precipitation may become less effective in maintaining soil moisture balance.

The U.S.'s highly urbanized population—nearly 80% living in cities—faces disproportionate drought exposure. By integrating drought classifications (D0-D4) from the ScPDSI, SPI-12, and SPEI-12 with gridded population projections, we find that urban areas consistently bear greater drought impacts than rural areas, particularly for the milder categories (D0-D1). Exposure peaks around 2030-2040 and declines towards 2050, with notable differences across indices. Under SPI-12, drought exposure peaks at 2.7 million people in 2030 and drops to 800 000 by 2050. In contrast, ScPDSI indicates more prolonged exposure, with 3.6 million affected in 2030 and 1.1 million still impacted by 2050. These differences reflect how precipitation-based (SPI-12), temperature-sensitive (SPEI-12), and soil moisturedriven (ScPDSI) indices yield different drought projections. Historically, urban populations have been more vulnerable to drought than rural areas, and this trend is expected to continue under SSP5-8.5 (figure 5). In 2010, 6.6 million urban residents experienced D0-D4 droughts compared to 1.1 million rural residents (SPI-12). ScPDSI estimated 3.5 million affected, compared to 2.1 million under SPI-12, highlighting differences in index sensitivity. By 2030, urban exposure peaks at 6.4 million under SPI-12 and 3.6 million under ScPDSI. Although numbers decline by 2050, ScPDSI continues to show more prolonged exposure, reinforcing concerns about persistent soil moisture deficits.

For D0 conditions under SPI-12, urban drought exposure rises from 1.76 million in 2010 to a peak of 2.46 million in 2030, then declines to 0.96 million by 2050. During the same period, rural exposure decreases from 0.35 million to just 0.1 million. ScPDSI estimates an even higher D0 exposure, with 3.2 million urban residents affected in 2030 and 1.1 million in 2050. Moderate drought (D1) follows a similar pattern, peaking at 1.24 million urban residents in 2030 (SPI-12) and decreasing to 0.14 million in rural areas by 2050. The ScPDSI estimates are more persistent, with urban D1 exposure at 2.5 million in 2030 and 1.3 million in 2050, reinforcing the role of long-term soil moisture deficits in sustaining droughts. For severe droughts (D2-D4), the decline is more pronounced. D2 affects 420 000 urban residents in 2030 (SPI-12) and 1.4 million in ScPDSI, but drops to 63 000 (SPI-12) and 437 000 (ScPDSI) by 2050. D3 peaks at 84 000 (SPI-12) and 101 000 (ScPDSI) in 2030, declining to 28 000 (SPI-12) and 90 000 (ScPDSI) by 2050. D4 remains the



least affected category, with urban exposure slightly increasing from 1321 in 2030 to 5141 in 2050 (SPI-12), while ScPDSI projects a larger but still small urban D4 population of 9 000 by 2050. These findings reinforce the persistent vulnerability of urban populations to long-term drought exposure under climate change (see supplementary figure S2 for population growth trends in urban and rural areas).

4. Discussion

We examined future drought dynamics across the CONUS using three complementary indices—SPI-12, SPEI-12, and ScPDSI—which reflect precipitation variability, temperature-driven evapotranspiration, and long-term soil moisture balance, respectively. The results show divergent trends: SPI-12 and SPEI-12 point to interannual fluctuations and a decrease in drought-affected areas by midcentury, while ScPDSI projects persistent soil moisture deficits, particularly in the Southwest. This divergence highlights the value of using multiple drought indices to capture the full range of drought processes under climate change. One limitation of this analysis is the use of a six-model ensemble under a single scenario (SSP5-8.5), with 10 year time slices that limit the reliability of extreme drought (D3-D4) projections. While SPI-12 and SPEI-12 show a median decline in D3-D4 droughts, ScPDSI projects that some regions may still face extended dry periods after 2050. This highlights that while the number of extreme droughts may decrease, persistent soil moisture deficits could continue to threaten water resources and agriculture. Expanding multi-scenario and multi-model ensembles would improve projection and better quantify future drought extremes. While our results diverge in some areas from coarse-resolution CMIP6 studies, this is expected given the additional processlevel detail captured through dynamical downscaling. RegCM4 preserves large-scale circulation signals from the driving GCMs while explicitly resolving regional features such as terrain-driven precipitation, mesoscale convection, and land-atmosphere interactions. These localized processes strongly influence drought behavior but are often absent in coarse models. The divergence is not due to model pre-selection. The six GCMs used were selected based on data availability, historical performance, and representation of a wide range of climate sensitivities (supplement text S2). Our findings therefore reflect physically meaningful improvements in regional drought representation rather than methodological inconsistencies.

We assessed projection reliability by examining the effects of dynamical downscaling, which explicitly resolves fine-scale climate processes in contrast to statistical approaches. This approach is particularly important in topographically complex areas like the western U.S., where GCMs often underestimate local precipitation variability and convective processes. Bias correction using Daymet V4 helped reduce systematic biases in temperature and precipitation, thereby improving the performance of temperature-sensitive drought indices such as SPEI and ScPDSI. The enhanced spatial resolution provides a more accurate representation of temperature-driven drought patterns. While raw GCM-based projections smooth out fine-scale drought patterns, our downscaled dataset provides a more detailed spatial representation of drought persistence and intensity across different climate zones. Despite improvements in downscaling, some biases persist. While precipitation biases in the Southwest have been reduced compared to raw GCM outputs, there is still a slight underestimation of extreme precipitation events, indicating the need for further refinement in hydrological applications. Similarly, temperature biases in RegCM4-based datasets were lower than those in raw GCMs, improving the reliability of temperature-sensitive drought indices. Overall, these findings demonstrate the usefulness of dynamical downscaling in improving the accuracy of regional drought projections. Although our downscaled ensemble enhances the spatial realism of drought projections, it does not eliminate uncertainty, which remains a fundamental aspect of future climate assessments. Model agreement improves in regions with strong geographic controls, such as the Southwest, while greater spread persists in areas like

the Midwest. This reflects both inherited variability from GCMs and methodological differences introduced during downscaling. Prior studies have shown that different techniques can produce notably different estimates of hydroclimatic extremes (Rastogi *et al* 2022). Figure 3 illustrates this spread using the 10th, 50th, and 90th percentiles. These results emphasize the value of regional modeling while underscoring the need for broader ensemble exploration.

Several recent studies using CMIP6 models have projected widespread intensification of drought severity under future high-emission scenarios based on SPEI indices (Zhao and Dai 2022, Zhou et al 2023, Niu et al 2025). While our findings may appear to differ, these discrepancies are primarily due to differences in methodological design. Many of the referenced studies use global-scale SPEI-3 derived from raw CMIP6 outputs at coarse spatial resolutions, which tend to emphasize short-term drought responses to warming. In contrast, our analysis applies bias-corrected, dynamically downscaled projections at 4 km resolution across the CONUS and focuses on SPEI-12, which reflects seasonal-to-annual water balance more relevant to long-term hydrological and agricultural impacts. As shown in figure S3, longer accumulation periods like SPEI-12 smooth short-term fluctuations and better capture persistent drought signals, while SPEI-3 displays more frequent and abrupt variability. Additionally, our indices are standardized to a consistent 1980-2019 baseline across the same spatial domain, reducing inconsistencies that may arise from global reference periods. As a result, our findings highlight increasing mild-tomoderate drought, particularly in the Southwest and urban areas, with fewer extreme drought events in some regions by mid-century. These results complement, rather than contradict, broader global assessments and underscore the importance of spatial resolution, drought timescale, and reference period in shaping projected drought trajectories.

Our findings align with previous studies showing a decline in drought in parts of CONUS, particularly the Upper Midwest and Southeast, due to projected increases in precipitation (Xue and Ullrich 2022, Chen and Ford 2023). In contrast, drought conditions in the Southwest and Western U.S. (e.g. New Mexico, Arizona, California) are expected to worsen as rising temperatures and evapotranspiration intensify soil moisture deficits (Heim 2017, Leeper et al 2022, Rastogi et al 2023). The role of rising temperatures in drought indices varies depending on the PET calculation method. SPEI explicitly accounts for temperature through PET and often employs the Thornthwaite method, which is highly sensitive to warming but does not consider vegetation responses to elevated CO₂ levels. ScPDSI incorporates temperature effects indirectly through soil moisture balance but does not fully

reflect CO₂-driven changes in PET. While Penman–Monteith PET is physically robust, it excludes CO₂-induced stomatal closure, which may lead to overestimation of future drying (Yang *et al* 2019). Future research should explore CO₂-sensitive PET models to better capture plant water use efficiency and drought severity under increasing CO₂ levels.

Although the total drought-affected population is projected to decrease by 2050, urban areas will remain disproportionately burdened by mild and moderate droughts due to their higher population density and location in persistently dry regions. However, projections vary across the drought indices: SPI-12 estimates a decrease in affected population from 2.7 million in 2030 to 0.8 million in 2050, while ScPDSI suggests a more prolonged impact, with 3.6 million affected in 2030 and 1.1 million in 2050. This suggests that while short-term precipitation variability may provide relief in some regions, longer-term soil moisture depletion remains a key concern. The findings emphasize the socioeconomic vulnerability of urban populations, particularly disadvantaged groups, in drought-prone areas (Liggett 2023). To address persistent drought risks, effective adaptation strategies are essential—such as improving water conservation, investing in resilient urban infrastructure, and expanding water reuse technologies. It is also important to acknowledge that population exposure estimates are based on a single socioeconomic scenario (SSP5-8.5), which introduces its own uncertainty. Future demographic shifts, migration, and policy changes could lead to alternative exposure outcomes. While SSP5 provides a high-growth, highemission baseline for stress-testing drought vulnerability, incorporating multiple SSPs in future work could better constrain the uncertainty range in projected human exposure to drought.

From an agricultural perspective, the indices reveal significant risks associated with shifting drought patterns. SPI-12 indicates a long-term trend toward reduced drought severity after 2040 (figure 1), suggesting fewer prolonged precipitation deficits, which may reduce water stress in some regions but pose challenges for rainfed agriculture that depends on consistent moisture availability (Harp and Horton 2022). In contrast, ScPDSI predicts persistent soil moisture deficits in the Southwest, where drought risk remains high even by 2050. Projected increases in precipitation may not fully offset soil moisture deficits, which could continue to affect crop resilience and yields (Ficklin et al 2015). More intense but less frequent precipitation events could complicate irrigation planning and disrupt crop schedules, even in regions projected to become wetter (Leeper et al 2022, Rastogi et al 2023). Agricultural systems must prepare for both more frequent mild droughts and

the increased baseline water stress they impose (Wahl *et al* 2022).

To calculate PET, this study used the Penman-Monteith method with the VIC hydrological model and bias-corrected GCM output, which is widely accepted for hydrological studies (Lang et al 2017, Goh et al 2021). The VIC-derived PET was subsequently used as the climatic input for the SPEI and ScPDSI calculations, thereby improving the physical realism of the index. Although ScPDSI has been criticized for its simplified soil moisture parameterization (Vicente-Serrano et al 2011), the use of physically based and validated PET helps to improve the credibility of its drought projections. The bias-corrected RegCM4 inputs driving the VIC model have been demonstrated to significantly improve temperature and precipitation representation across CONUS, particularly in the Southwest (Rastogi et al 2022), see also in supplementary text S3). However, limitations such as temporal uncertainties and energy balance closure issues may introduce biases in drought index calculations (Hao et al 2018a). Additionally, the modifiable areal unit problem complicates results, even when dividing the CONUS into NCEI climate regions to align with previous studies (Jelinski and Wu 1996, Ashfaq et al 2016). In addition, different drought classification thresholds, such as -0.5 for SPI/SPEI and -1 for ScPDSI, influence the areas and populations identified as drought-affected (Maule et al 2013, Nam et al 2015, Chivangulula et al 2023). Although our study follows conventional classification criteria, nonparametric methods offer a consistent framework for comparing drought indices across variables, improving cross-index comparability (Farahmand and AghaKouchak 2015). These methodological challenges emphasize the need for standardized approaches to improve consistency and reliability in drought assessments.

5. Conclusion

This study presents a high-resolution, multi-model assessment of future drought trends across CONUS and their population impacts under the SSP5-8.5 scenario. The results reveal a growing regional disparity. While areas like the Upper Midwest and Northeast may see fewer droughts due to increased precipitation, the Southwest and Western U.S.—including New Mexico, Arizona, and California—are projected to face persistent and intensifying droughts driven by rising temperatures and long-term soil moisture deficits. By integrating multiple drought indices (SPI-12, SPEI-12, and ScPDSI), this study highlights the need to capture both short-term precipitation variability and long-term hydrological stress to fully understand evolving drought risks. Although

the total population affected by drought is expected to decrease by mid-century, urban areas remain disproportionately vulnerable, especially to mild-tomoderate drought (D0-D1). For example, SPI-12 estimates that 0.96 million urban residents will face D0 conditions by 2050—down from 1.76 million in 2010. In contrast, ScPDSI projects more prolonged exposure, with 3.2 million affected in 2030 and 1.1 million in 2050. Urban expansion in droughtprone regions like the Southwest and Southern California may heighten socioeconomic vulnerability. Addressing these challenges requires targeted strategies—such as resilient water infrastructure, sustainable irrigation, and drought-tolerant agriculture. Future research should incorporate CO₂-responsive PET models and dynamic vegetation feedback to better capture plant physiological responses under climate change. It is important to recognize that the study is based on a relatively small ensemble of six models under a single climate scenario (SSP5-8.5), with drought trends analyzed over 10 year time slices. While the findings offer valuable insights into regional drought trends, the limited sample size constrains the detection of robust trends in extreme events. Future research using larger model ensembles, multiple scenarios, and longer timeframes is needed to strengthen the robustness of projections.

Data availability statement

All the CMIP6 GCMs data are publicly available (from https://esgf-node.llnl.gov/projects/cmip6/). All data analysis was done using the R programming language (RDevelopment Core Team 2011), Python (Van Rossum and Drake 1995)and Climate Data Operators (Schulzweida 2023). The source code for RegCM4 is available online (from https://github.com/ICTP/RegCM). A non-github version cannot be provided since the code is maintained by a separate organization (International Centre for Theoretical Physics, Trieste, Italy).

All data that support the findings of this study are included within the article (and any supplementary files).

Acknowledgment

This research used resources of the Oak Ridge Leadership Computing Facility at the Oak Ridge National Laboratory, which is supported by the Office of Science of the U.S. Department of Energy under Contract No. DE-AC05-00OR22725. This research also used resources of the National Energy Research Scientific Computing Center, which is supported by the Office of Science of the U.S. Department of Energy under Contract No. DE-AC02-05CH11231.

Author contributions

J S F and L Z conceptualized the study. D R, S-C K, and M A provided and verified the model data. L Z, H J R and R-Y C developed the methodology and did the data analysis. L Z created the data visualizations and wrote the original draft. H J R, R-Y C, J S F, D R, S-C K, and M A reviewed and edited the manuscript.

Conflict of interest

The authors declare no conflict of interest.

ORCID iDs

Leyuan Zhang © 0000-0003-1148-7312 Hannah J Rubin © 0000-0001-8222-6924 Rong-You Chien © 0009-0008-0204-1996 Joshua S Fu © 0000-0001-5464-9225 Deeksha Rastogi © 0000-0002-0462-4027 Shih-Chieh Kao © 0000-0002-3207-5328 Moetasim Ashfaq © 0000-0003-4106-3027

References

Agnew C T 2000 Using the SPI to identify drought *Drought Netw.* News $12\,6$ –12

Ashfaq M, Rastogi D, Mei R, Kao S-C, Gangrade S, Naz B S and Touma D 2016 High-resolution ensemble projections of near-term regional climate over the continental United States J. Geophys. Res. 121 9943–63

Beguería S, Vicente-Serrano S M, Reig F and Latorre B 2014 Standardized precipitation evapotranspiration index (SPEI) revisited: parameter fitting, evapotranspiration models, tools, datasets and drought monitoring *Int. J. Climatol.* 34 3001–23

Chang J, Li Y, Wang Y and Yuan M 2016 Copula-based drought risk assessment combined with an integrated index in the Wei River Basin, China *J. Hydrol.* **540** 824–34

Chen L and Ford T W 2023 Future changes in the transitions of monthly-to-seasonal precipitation extremes over the Midwest in Coupled Model Intercomparison Project Phase 6 models Int. J. Climatol. 43 255–74

Chiang F, Mazdiyasni O and AghaKouchak A 2018 Amplified warming of droughts in southern United States in observations and model simulations *Sci. Adv.* **4** eaat2380

Chivangulula F M, Amraoui M and Pereira M G 2023 The drought regime in Southern Africa: a systematic review Climate 11 147

Coppola E, Stocchi P, Pichelli E, Torres Alavez J A, Glazer R, Giuliani G, Di Sante F, Nogherotto R and Giorgi F 2021 Non-hydrostatic RegCM4 (RegCM4-NH): model description and case studies over multiple domains Geosci. Model Dev. 14 7705–23

Covich A P, Crowl T A, Hein C L, Townsend M J and Mcdowell W H 2009 Predator–prey interactions in river networks: comparing shrimp spatial refugia in two drainage basins *Freshwater Biol.* 54 450–65

Dai A and Zhao T 2017 Uncertainties in historical changes and future projections of drought. Part I: estimates of historical drought changes *Clim. Change* 144 519–33

Eyring V, Bony S, Meehl G A, Senior C A, Stevens B, Stouffer R J and Taylor K E 2016 Overview of the Coupled Model Intercomparison Project Phase 6 (CMIP6) experimental design and organization *Geosci. Model Dev.* 9 1937–58

- Falloon P et al 2018 The land management tool: developing a climate service in Southwest UK Clim. Serv. 9 86–100
- Farahmand A and AghaKouchak A 2015 A generalized framework for deriving nonparametric standardized drought indicators *Adv. Water Resour.* **76** 140–5
- Ficklin D L, Maxwell J T, Letsinger S L and Gholizadeh H 2015 A climatic deconstruction of recent drought trends in the United States Environ. Res. Lett. 10 044009
- Giorgi F 2019 Thirty years of regional climate modeling: where are we and where are we going next? *J. Geophys. Res.* 124 5696–723
- Goh E H, Ng J L, Huang Y F and Yong S L S 2021 Performance of potential evapotranspiration models in Peninsular Malaysia J. Water Clim. Change 12 3170–86
- Hao X, Zhang S, Li W, Duan W, Fang G, Zhang Y and Guo B 2018a The uncertainty of Penman–Monteith method and the energy balance closure problem *J. Geophys. Res.* 123 7433–43
- Hao Z, Singh V P and Xia Y 2018b Seasonal drought prediction: advances, challenges, and future prospects Rev. Geophys. 56 108–41
- Harp R D and Horton D E 2022 Observed changes in daily precipitation intensity in the United States *Geophys. Res. Lett.* **49** e2022GL099955
- Hayes M, Svoboda M D, Wardlow B D, Anderson M and Kogan F 2012 Drought monitoring: historical and current perspectives (Drought Mitigation Center: Faculty Publications) (available at: https://digitalcommons.unl.edu/ droughtfacpub/94)
- Heim R R 2002 A review of twentieth-century drought indices used in the United States *Bull. Am. Meteorol. Soc.* 83 1149–66
- Heim R R 2017 A comparison of the early twenty-first century drought in the United States to the 1930s and 1950s drought episodes *Bull. Am. Meteorol. Soc.* 98 2579–92
- Hoffmann D, Gallant A J and Arblaster J M 2020 Uncertainties in drought from index and data selection J. Geophys. Res. Atmos. 125
- Hu Y-M, Liang Z-M, Liu Y-W, Wang J, Yao L and Ning Y 2015 Uncertainty analysis of SPI calculation and drought assessment based on the application of bootstrap *Int. J. Climatol.* 35 1847–57
- Jelinski D E and Wu J 1996 The modifiable areal unit problem and implications for landscape ecology *Landscape Ecol*. 11 129–40
- Jones B and O'Neill B C 2016 Spatially explicit global population scenarios consistent with the shared socioeconomic pathways Environ. Res. Lett. 11 084003
- Jones B, O'Neill B C and Gao J 2020 Global 1-km Downscaled Population Base Year and projection grids for the shared socioeconomic pathways (SSPs) revision 01 (available at: https://sedac.ciesin.columbia.edu/data/set/popdynamics-1-km-downscaled-pop-base-year-projection-ssp-2000-2100-rev01)
- Karl T R 1983 Some spatial characteristics of drought duration in the United States J. Appl. Meteorol. Climatol. 22 1356–66
- Lang D, Zheng J, Shi J, Liao F, Ma X, Wang W, Chen X and Zhang M 2017 A comparative study of potential evapotranspiration estimation by eight methods with FAO Penman–Monteith method in Southwestern China Water 9 734
- Leeper R D, Bilotta R, Petersen B, Stiles C J, Heim R, Fuchs B, Prat O P, Palecki M and Ansari S 2022 Characterizing U.S. drought over the past 20 years using the U.S. Drought Monitor *Int. J. Climatol.* 42 6616–30
- Li M, Cao F, Wang G, Chai X and Zhang L 2020 Evolutional characteristics of regional meteorological drought and their linkages with southern oscillation index across the loess plateau of China during 1962–2017 *Sustainability* 12 7237
- Liggett A 2023 NCA5: drought and Climate Change in 10 Maps (Climate Program Office) (available at: https://cpo.noaa.gov/nca5-drought-and-climate-change-in-10-maps/)

- Littell J S, Peterson D L, Riley K L, Liu Y and Luce C H 2016 A review of the relationships between drought and forest fire in the United States Glob. Change Biol. 22 2353–69
- Maule C F, Thejll P, Christensen J H, Svendsen S H and Hannaford J 2013 Improved confidence in regional climate model simulations of precipitation evaluated using drought statistics from the ENSEMBLES models Clim. Dyn. 40 155–73
- McEnery J, Ingram J, Duan Q, Adams T and Anderson L 2005 NOAA's advanced hydrologic prediction service: building pathways for better science in water forecasting *Bull. Am. Meteorol. Soc.* **86** 375–86
- McKee T B, Doesken N J and Kleist J 1993 The relationship of drought frequency and duration to time scales *Proc. 8th Conf. on Applied Climatology (Anaheim, CA, 17–22 January* 1993) (American Meteorological Society) pp 179–84
- Mishra A K and Singh V P 2010 A review of drought concepts *J. Hydrol.* 391 202–16
- Mülmenstädt J and Wilcox L J 2021 The fall and rise of the global climate model *J. Adv. Model. Earth Syst.* 13 e2021MS002781
- Nam W-H, Hayes M J, Svoboda M D, Tadesse T and Wilhite D A 2015 Drought hazard assessment in the context of climate change for South Korea *Agric. Water Manage.* **160** 106–17
- Niu Q, She D, Xia J, Zhang Q, Zhang Y and Wang T 2025 Uncertainty analysis of global meteorological drought in CMIP6 projections *Clim. Change* **178** 75
- O'Neill B C *et al* 2016 The scenario model intercomparison project (ScenarioMIP) for CMIP6 *Geosci. Model Dev.* 9 3461–82
- Palmer W C 1965 *Meteorological Drought* (U.S. Department of Commerce, Weather Bureau)
- Qiu Y, Feng J, Yan Z, Wang J and Li Z 2022 High-resolution dynamical downscaling for regional climate projection in Central Asia based on bias-corrected multiple GCMs *Clim. Dyn.* **58** 777–91
- Raju K S and Kumar D N 2020 Review of approaches for selection and ensembling of GCMs J. Water Clim. Change 11 577–99
- Rastogi D, Kao S-C and Ashfaq M 2022 How may the choice of downscaling techniques and meteorological reference observations affect future hydroclimate projections? *Earth's Future* 10 e2022EF002734
- Rastogi D, Trok J, Depsky N, Monier E and Jones A 2023 Historical evaluation and future projections of compound heatwave and drought extremes over the conterminous United States in CMIP6* *Environ. Res. Lett.* **19** 014039
- RDevelopment Core Team 2011 R: a language and environment for statistical computing (R Foundation for Statistical Computing Team)
- Rippey B R 2015 The U.S. drought of 2012 Weather Clim.

 Extremes 10 57–64
- Schulzweida U 2023 CDO user guide (available at: https://zenodo. org/records/10020800)
- Smith A B 2020 U.S. Billion-dollar Weather and climate disasters, 1980—present (NCEI accession 0209268) (available at: www.ncei.noaa.gov/archive/accession/0209268)
- Sugg M et al 2020 A scoping review of drought impacts on health and society in North America Clim. Change 162 1177–95
- Svoboda M et al 2002 THE DROUGHT MONITOR Bull. Am. Meteorol. Soc. 83 1181–90
- Thornton M M, Shrestha R, Wei Y, Thornton P E and Kao S-C 2022 Daymet: Daily surface weather data on a 1-km grid for North America, Version 4 R1 ORNL DAAC Oak Ridge, Tennessee, USA (https://doi.org/10.3334/ORNLDAAC/2129)
- Van Rossum G and Drake F L 1995 *Python Reference Manual* vol 111 (Centrum voor Wiskunde en Informatica Amsterdam) (available at: www.cs.cmu.edu/afs/cs.cmu.edu/project/ gwydion-1/OldFiles/OldFiles/python/Doc/ref.ps)
- Vicente-Serrano S M, Beguería S and López-Moreno J I 2010 A multiscalar drought index sensitive to global warming: the standardized precipitation evapotranspiration index *J. Clim.* **23** 1696–718

- Vicente-Serrano S M, López-Moreno J I, Gimeno L, Nieto R, Morán-Tejeda E, Lorenzo-Lacruz J, Beguería S and Azorin-Molina C 2011 A multiscalar global evaluation of the impact of ENSO on droughts J. Geophys. Res. 116 D24107
- Wahl E R, Zorita E, Diaz H F and Hoell A 2022 Southwestern United States drought of the 21st century presages drier conditions into the future Commun. Earth Environ. 3 1–14
- Wang H, Pan Y and Chen Y 2017a Comparison of three drought indices and their evolutionary characteristics in the arid region of northwestern China *Atmos. Sci. Lett.* **18** 132–9
- Wang Y, Xie Y, Dong W, Ming Y, Wang J and Shen L 2017b Adverse effects of increasing drought on air quality via natural processes *Atmos. Chem. Phys.* 17 12827–43
- Xue Z and Ullrich P A 2022 Changing trends in drought patterns over the Northeastern United States using multiple large ensemble datasets J. Clim. 35 7413–33
- Yang Y, Roderick M L, Zhang S, McVicar T R and Donohue R J 2019 Hydrologic implications of vegetation response to

- elevated CO₂ in climate projections *Nat. Clim. Change* 9 44–48
- Zhang L, Wang Y, Chen Y, Bai Y and Zhang Q 2020 Drought risk assessment in central Asia using a probabilistic copula function approach *Water* 12 421
- Zhao B, Kao S-C, Zhao G, Gangrade S, Rastogi D, Ashfaq M and Gao H 2023 Evaluating enhanced reservoir evaporation losses from CMIP6-based future projections in the contiguous United States *Earth's Future* 11 e2022EF002961
- Zhao T and Dai A 2022 CMIP6 model-projected hydroclimatic and drought changes and their causes in the twenty-first century (available at: https://journals.ametsoc.org/view/journals/clim/35/3/JCLI-D-21-0442.1.xml)
- Zhong Z, He B, Guo L and Zhang Y 2019 Performance of various forms of the palmer drought severity index in China from 1961 to 2013 *J. Hydrometeorol.* 20 1867–85
- Zhou Z, Zhang L, Chen J, She D, Wang G, Zhang Q, Xia J and Zhang Y 2023 Projecting global drought risk under various SSP-RCP scenarios *Earth's Future* 11 e2022EF003420